View metadata, citation and similar papers at core.ac.uk

brought to you by CORE

provided by Publications at Bielefeld University

Report

Current Biology

Feeling a Touch to the Hand on the Foot

Highlights

- Healthy adults misattributed touch from hands to feet and vice versa
- Erroneously reported limbs were of the same body side and type as the touched limb
- Further, limbs were erroneously chosen based on their position in external space
- However, the touch's external-spatial location was irrelevant

Authors

Stephanie Badde, Brigitte Röder, Tobias Heed

Correspondence

stephanie.badde@nyu.edu

In Brief

Badde et al. find that healthy adults misattribute touch across hands and feet. These misattributions replicate across five experiments, and modeling links them to perceptual, rather than decision-making, processes. Error patterns reveal that humans disregard the position of a touch in space and use anatomical information when identifying a touched limb.

Badde et al., 2019, Current Biology *29*, 1–7
May 6, 2019 © 2019 Elsevier Ltd.
https://doi.org/10.1016/j.cub.2019.02.060

CellPress

Please cite this article in press as: Badde et al., Feeling a Touch to the Hand on the Foot, Current Biology (2019), https://doi.org/10.1016/j.cub.2019.02.060

Current Biology
Report

CellPress

Feeling a Touch to the Hand on the Foot

Stephanie Badde,[1,2,5,*] Brigitte Röder,[2] and Tobias Heed[3,4]
[1]Department of Psychology and Center of Neural Sciences, New York University, 6 Washington Place, New York, NY 10003, USA
[2]Biological Psychology and Neuropsychology, University of Hamburg, Von-Melle-Park 11, 20146 Hamburg, Germany
[3]Biopsychology & Cognitive Neuroscience, Bielefeld University, Universitätsstrasse 25, 33615 Bielefeld, Germany
[4]Center of Excellence Cognitive Interaction Technology (CITEC), Bielefeld University, Inspiration 1, 33619 Bielefeld, Germany
[5]Lead Contact
*Correspondence: stephanie.badde@nyu.edu
https://doi.org/10.1016/j.cub.2019.02.060

SUMMARY

Where we perceive a touch putatively depends on topographic maps that code the touch's location on the skin [1] as well as its position in external space [2–5]. However, neither somatotopic nor external-spatial representations can account for atypical tactile percepts in some neurological patients and amputees; referral of touch to an absent or anaesthetized hand after stimulation of a foot [6, 7] or the contralateral hand [8–10] challenges the role of topographic representations when attributing touch to the limbs. Here, we show that even healthy adults systematically misattribute touch to other limbs. Participants received two tactile stimuli, each to a different limb—hand or foot—and reported which of all four limbs had been stimulated first. Hands and feet were either uncrossed or crossed to dissociate body-based and external-spatial representations [11–14]. Remarkably, participants regularly attributed the first touch to a limb that had received neither of the two stimuli. The erroneously reported, non-stimulated limb typically matched the correct limb with respect to limb type or body side. Touch was misattributed to non-stimulated limbs of the other limb type and body side only if they were placed at the correct limb's canonical (default) side of space. The touch's actual location in external space was irrelevant. These errors replicated across several contexts, and modeling linked them to incoming sensory evidence rather than to decision strategies. The results highlight the importance of the touched body part's identity and canonical location but challenge the role of external-spatial tactile representations when attributing touch to a limb.

RESULTS

Participants received two successive, supra-threshold vibrotactile stimuli, each to a different, randomly selected limb—hand or foot. They identified the limb stimulated first and responded by a button press with that limb. Usually, participants indicated the correct limb or the limb stimulated second. However, they also regularly reported limbs that had not received either touch. For instance, they responded with a foot after stimulation of the two hands or with a left limb after stimulation of the two right limbs. We refer to these responses as phantom errors, given that the indicated limb had not received peripheral input. To determine the factors that governed these tactile misattributions, we analyzed whether the reported (phantom error) and the correct (first touch) limb corresponded with respect to their limb type, body side, and external-spatial location (Figures 1A and 1B).

Here, we focus on phantom errors, that is, misattributions of touch toward non-stimulated limbs. Since these occurred at low rates (8% of trials), we employed Poisson models for their quantitative analysis. The reported beta weights indicate the predicted difference in phantom-error counts between the compared conditions in log-units.

Phantom Errors Vary with Limb Type and Posture of the Correct Limb

First, we tested whether participants represented the stimulated limb with respect to its type (hand or foot) by contrasting the frequency of misattributions toward limbs of the same (homologous; Figure 1B, dashed, open-head arrows) and other (non-homologous) type as the correct limb. Confusions between crossed, homologous limbs were especially frequent (Figure 1C, gray bars; posture correct limb × limb-type homology, $\beta = 0.43$, $p < 0.001$; see Data S1A for full models of data from this and subsequent experiments). For instance, participants attributed touch to the right hand more often to the non-stimulated left hand when the hands were crossed than when they were uncrossed. Misattributions toward the homologous limb were more prominent for the feet than for the hands for both crossed (type, correct limb, $\beta = 1.02$, $p < 0.001$) and uncrossed ($\beta = 0.38$, $p < 0.001$, Figure 1C, gray bars, lower versus upper part) postures. When participants misattributed touch toward a non-homologous limb, foot-instead-of-hand errors occurred as often as (uncrossed, $\beta = 0.00$, $p = 0.929$) or more often than (crossed, $\beta = 0.31$, $p < 0.001$) hand-instead-of-foot errors (Figure 1C, purple bars, upper versus lower part).

The frequent misattribution of touch to the non-stimulated homologous limb (Figure 1C, gray bars) suggests that participants used the type of the touched limb to represent tactile locations. Yet, the modulation of phantom errors by posture, as well as misattributions toward non-homologous limbs (Figure 1C, purple bars), shows that additional factors must play a role when one attributes touch to a limb.

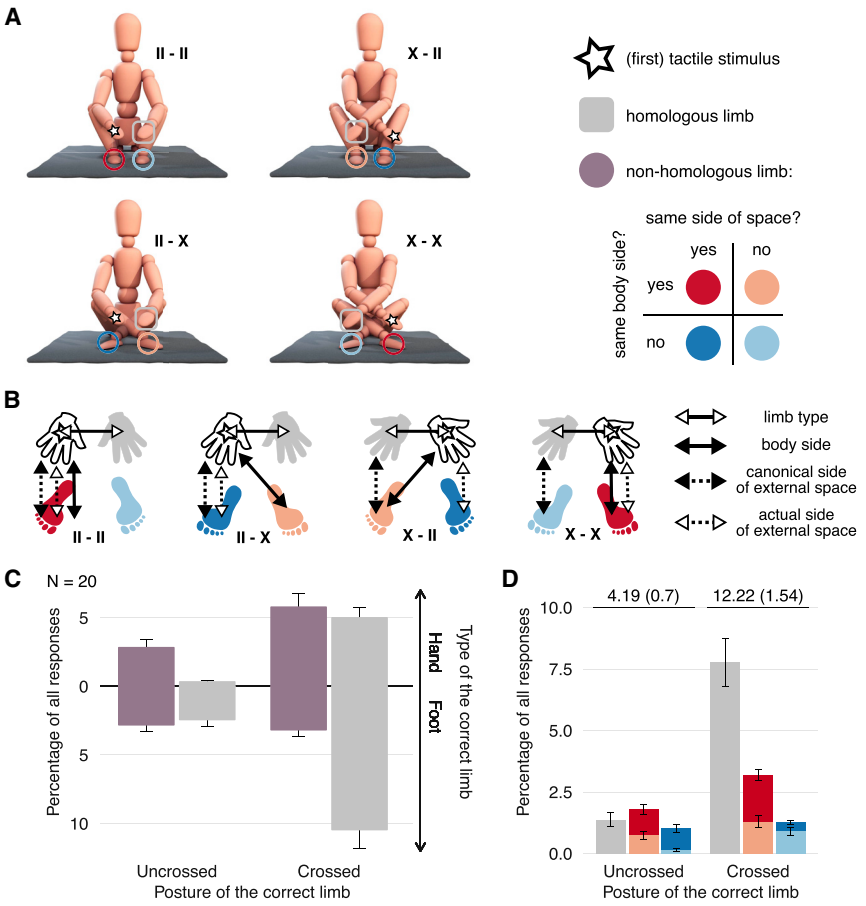

Figure 1. Experimental Design and Results of Experiment 1

(A) Participants sat on the floor and rested their hands on transparent platforms 20 cm above their feet. Hands and feet were either uncrossed (II) or crossed (X). Each limb was equipped with a tactile stimulator and a response button. In every trial, two different, randomly selected limbs were stimulated in rapid succession. Instructions were to respond by button press with the limb that received the first touch. Most responses were either made with the correct limb (white star) or the limb stimulated second. Yet, participants frequently reported limbs that had not been stimulated, responses we refer to as phantom errors. Compared to the correct limb, which is the limb stimulated first, the erroneously identified limb could be of the same (homologous limb, gray) or the other (non-homologous limb, purple) limb type, from the same (red shades) or the other (blue shades) body side, and placed at the same (darker colors) or the other (brighter colors) side of external space. The colored circles illustrate these different categories of phantom errors in the four postures in the case of a touch to the right hand.

(B) Predicted activation of each of the four limbs after tactile stimulation of the right hand, shown for the four posture conditions and from the same perspective as in (A). The predicted activations are based on different spatial representations of the touched limb: its limb type (solid, open-head arrow), its body side (solid, closed-head arrow), its (accurate) side of external space (dotted, open-head arrow), and its canonical (default) side of external space (dotted, closed-head arrow). Each spatial representation predicts activation of two different limbs; not all of the predictions were met by phantom errors, see (D) and Results.

(C) Percentage of responses that are phantom errors as a function of the initially stimulated limb's type and posture, separated into misattributions of touch to homologous (gray) and non-homologous (purple) limbs.

(D) Phantom-error frequencies (relative to all responses) per posture of the correct limb as a function of the correspondences between correct and responding limbs listed in (A). Bars are stacked so that each bar is based on the same number of presented trials; see (A). The underlined text above the bars reports overall percentages per posture. Corresponding standard errors of the mean are in parentheses. Error bars indicate standard errors of the mean for the different phantom-error categories. See also Figure S1 and Data S1A and S1B.

Phantom Errors with Non-Homologous Limbs Predominantly Occur with Limbs from the Same Body Side as the Correct Limb

Each limb can be unambiguously described by its limb type and body side (the right hand or the left foot). To examine whether participants used body side to represent the touched limb, we tested whether touch was more often misattributed to limbs from the same body side as the correct limb (Figure 1B, solid, closed-head arrows) than to limbs from the other body side. To avoid a confound with limb type, only misattributions toward non-homologous limbs were considered for this analysis. Indeed, touch was more frequently misattributed to limbs from the same side than from the other body side as the correct limb (body side, uncrossed, $\beta = 0.46$, $p < 0.001$; crossed, $\beta = 0.49$, $p < 0.001$; Figure 1D, red versus blue bars). For example, a touch to the right hand was more likely misattributed to the right than to the left foot. Thus, participants represented the touched limb also with respect to its body side.

Phantom Errors with Non-Homologous Limbs Predominantly Occur with Limbs Placed at the Correct Limb's Canonical Side of External Space

Finally, we tested the role of external-spatial tactile representations by analyzing the frequency of phantom errors that could not be ascribed to limb-type- and body-side-based representations of the touched limb (Figure 1, dark and light blue). For touch to an uncrossed limb, phantom errors with the non-homologous limb placed at the correct limb's side of space were more frequent than with limbs placed at the other side of external space ($\beta = 0.54$, $p < 0.001$, Figure 1D uncrossed, dark versus light blue bar). A touch to the uncrossed right hand was misattributed to whichever foot was currently placed at the right side of external space. However, when an uncrossed limb is stimulated, two tactile spatial representations overlap: the actual external-spatial location of the touch and the canonical (default) external-spatial location of the touched limb (Figure 1B, II-II and II-X, dotted arrows). When touch is applied to crossed limbs, these two spatial representations

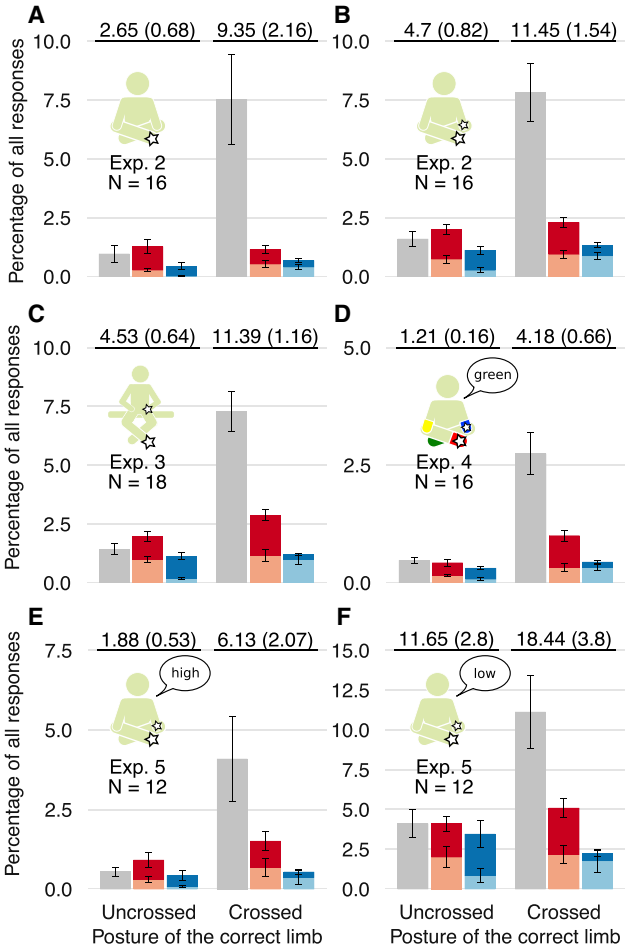

Figure 2. Phantom-Error Response Patterns across the Limbs: Experiments 2–5

(A and B) In experiment 2, trials randomly comprised either one (A) or two (B) tactile stimuli.

(C) In experiment 3, the vertical distance between hands and feet was increased from 20 to 70 cm.

(D) In experiment 4, participants wore colored sleeves and responded verbally by naming the sleeve color of the chosen limb.

(E and F) In experiment 5, participants indicated in each trial whether they had high (E) or low (F) confidence in the correctness of their limb choice response. Note that the reported percentages are relative to all responses, and responses other than phantom errors (correct responses and temporal order errors) were not split according to limb type, body side, and external space. For (E) and (F), all responses were, however, split according to their confidence rating (compare with Figure 3). Note further that the effects of body side and canonical side of external space are not additive (except in A); the critical pairwise comparisons are those conditions in which the other correspondence is absent (body side, uncrossed: light red versus light blue; crossed: dark red versus dark blue; canonical side of space, light blue versus dark blue, in opposite directions for uncrossed and crossed postures). Conventions are as in Figure 1.

correspond to opposite sides of external space (Figure 1B, X-II and X-X, dotted arrows). Phantom-error responses were more frequent with non-homologous limbs (of the other body side) placed at the correct limb's canonical side of external space than with limbs placed at the correct limb's actual side of external space ($\beta = 0.14$, $p < 0.001$, Figure 1C crossed, light versus dark blue bar). For instance, after stimulation of the crossed right hand, participants reported the foot placed at the right side, even though the touch was located at the left side of external space. Thus, touch was misattributed toward limbs placed at the correct limb's canonical side of external space, implying that not the touch but the reported limbs were represented external spatially.

The effects of canonical side of external space and body side (Figure 1A) were not additive (hemispace × body side, uncrossed, $\beta = 0.37$, $p < 0.001$; crossed, $\beta = 0.31$, $p < 0.001$). Yet, pairwise comparisons confirmed the influence of either factor in the absence of the other (Data S1B).

In sum, touch was misattributed toward limbs that matched the touched limb with respect to limb type, body side, and canonical rather than actual side of external space. Importantly, these three spatial representations account for the increase in misattributions toward homologous limbs with crossing as well (Figures 1C and 1D, gray bars). For instance, when the right hand is touched, limb type activates the two hands, body side activates the right hand and foot, and the canonical spatial representation activates limbs located at the right side of external space. Crossing the hands results in relatively more activation of the right than of the left hand, rendering left-hand responses unlikely (Figure 1B, II-II and II-X). When the hands are crossed, both limb type and the right hand's canonical hemispace activate the left hand, rendering left-hand responses more likely (Figure 1B, X-II and X-X).

Phantom-Error Patterns Are Unaffected by the Second Touch

The experiment involved two stimuli, which leads to more errors than do single-touch variants [15]. We examined whether timing and location of the second touch affected phantom errors. Phantom-error rates increased with decreasing time intervals between the two tactile stimuli, but the pattern of phantom errors remained stable (50 ms and 110 ms, Spearman's rho, $\rho = 0.964$, $p < 0.001$; 50 ms and 300 ms, $\rho = 0.867$, $p = 0.003$; 110 ms and 300 ms, $\rho = 0.939$, $p < 0.001$; experiments 2–5, see Data S1C). The analysis with respect to the relative location of the second touch (see STAR Methods for details) revealed no significant results (Data S1D). In sum, the pattern of phantom errors depended only on the location of the first touch.

Phantom Errors Occur Also When Only a Single Touch Is Presented

Next, we assessed whether phantom errors generalize across stimulation contexts. Experiment 2 closely resembled the first experiment, but now participants received only one tactile stimulus in half of the trials. Phantom errors in experiment 2 were distributed as in experiment 1 for both one-stimulus ($\rho = 0.903$, $p < 0.001$; Figure 2A; see Supplemental Information for Poisson models analogous to the analysis of experiment 1) and two-stimulus ($\rho = 0.975$, $p < 0.001$; Figure 2B) trials, though mean phantom-error rates were slightly lower in one-stimulus trials. Thus, the stimulation protocol (one or two stimuli per trial) was irrelevant for the pattern of phantom errors in both experiments. The second tactile stimulus possibly fosters phantom errors by interrupting processing of the first

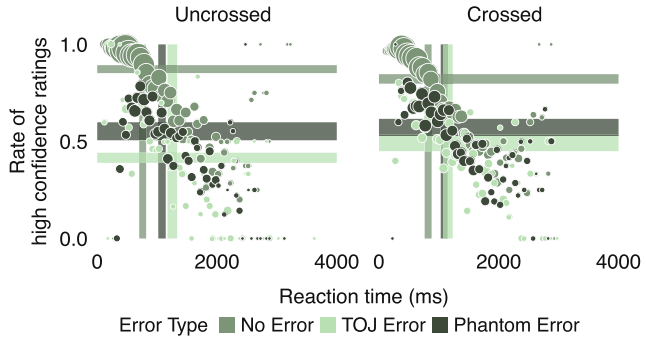

Figure 3. Confidence Ratings across Response Types and Reaction Time Bins in Experiment 5

The ratio of high to low confidence ratings. Circles indicate high confidence response rates by posture of the correct limb as a function of binned reaction times (50 ms binwidth) and by response type: correct responses (green), temporal order errors (reporting the limb stimulated second; dark green), and phantom errors (reporting a non-stimulated limb; light green). Circle sizes correspond to the average number of trials per condition. Horizontal bars indicate ± 1 SEM around the group's mean rate of high confidence ratings for each response type. Vertical bars indicate ± 1 SEM around group mean reaction times. See also Figure S2 and Data S1E.

touch [11, 16, 17], but if it does, it does so in a spatially unspecific manner.

Misattributions from Hand to Foot Are Invariant to Their External-Spatial Distance

In experiments 1 and 2, participants regularly reported touch to a hand at a non-stimulated foot and vice versa. To test whether these errors depended on the proximity of hands and feet, we varied their external-spatial distance. Experiment 3 repeated experiment 1, but the physical distance between hands and feet was increased from 20 to 70 cm. The pattern of phantom errors again closely replicated that of experiment 1 ($\rho = 0.903$, $p < 0.001$; Figure 2C), and the vertical distance between the limbs did not significantly modulate the effect of (canonical) side of space (experiment × hemispace, $\beta = 0.01$, $p = 0.780$). Thus, the external-spatial distance between hands and feet did not influence whether touch was misattributed to a non-homologous limb.

Phantom-Error Patterns Are Consistent, but Rates Decrease, When Participants Respond Verbally

Experiment 4 disentangled the role of perceptual and motor processes for phantom errors by removing the requirement for a spatial motor response. Participants wore differently colored sleeves and responded verbally by naming the color of the limb that received the first touch. Mean phantom-error rates dropped by half compared to those in the one-stimulus button-response task, while the pattern of phantom errors across limbs persisted ($\rho = 0.963$, $p < 0.001$; Figure 2D). The category-independent drop in phantom-error rates could indicate that analogous factors govern limb selection in tactile-perceptual and sensorimotor processing [18]; however, reaction times were longer for verbal responses than for button presses (Figure S2; Data S1E), suggesting a trade-off between speed and accuracy. Importantly, the consistent patterns across response modes imply that phantom errors have a perceptual component.

Participants Felt Similarly Confident about Misattributions toward Non-Stimulated and Stimulated Limbs

Experiment 5 tested whether phantom errors, which are responses indicating non-stimulated limbs, were associated with greater uncertainty than were temporal order errors, which are erroneous responses indicating the limb touched second. Participants reported their confidence (high or low) about having reported the correct limb after each button press. As is typical for confidence judgments, participants were significantly more confident about correct than about erroneous responses [19] (Figure 3; correct versus phantom error, $\beta = 7.55$, $p < 0.001$; correct versus temporal error, $\beta = 8.37$, $p < 0.001$), and more confident about fast than about slow responses [20, 21] ($\beta = -1.91$, $p < 0.001$). Critically, confidence ratings for phantom and temporal-order errors with similar response times were not significantly different (error type × RT, $\beta = 0.19$, $p = 0.229$; error type, $\beta = 0.85$, $p = 0.456$), suggesting that phantom errors were perceptually indistinguishable from errors with a touched limb. Confidence was not found to significantly vary with phantom-error category (Figures 2E and 2F). In summary, participants' confidence did not significantly differ between phantom errors and errors when reporting a touched limb, suggesting similar perceptual experiences.

Modeling Indicates That Phantom Errors Are Based on Perceptual Evidence

Finally, we examined putative mechanisms behind the emergence of phantom errors by modeling the accumulation of evidence for each limb, reflected in the relative response-time distributions of correct and erroneous responses [22]. To disentangle the roles of perceptual and decision processes, we probed model components representing each processing stage (see Figure 4 and STAR Methods for a detailed description). Model comparisons (Data S1F) favored a variant that attributed phantom errors to the perceptual stage. In the selected model, sensory evidence not only for the correct limb but also for a non-stimulated limb (e.g., of the same limb type) continually arrives at the decision stage. Most tactile spatial representations point toward the correct limb. Accordingly, on average, the sensory evidence signal of the stimulated limb is stronger, evidence accumulates more quickly, and the correct response is given. However, the strength of each limb's sensory evidence signal fluctuates randomly within and across trials, likely reflecting variations in the strength of the different spatial representations of the touched limb. Additionally, the four accumulators inhibit each other proportionally to their activation, leading to situations in which the accumulated evidence for one non-stimulated limb prevails and phantom errors arise. The combination of steadily incoming evidence toward a non-stimulated limb and trial-by-trial fluctuations in each evidence signal's base strength was critical for reproducing empirical phantom-error rates and reaction time distributions. In contrast, model fit was not improved by components that represent the decision stage: the possibility that phantom errors are based on less accumulated evidence than correct responses, that is, a collapsing decision threshold [26], was rejected. In sum, modeling gave strong support for perceptual accounts of phantom errors.

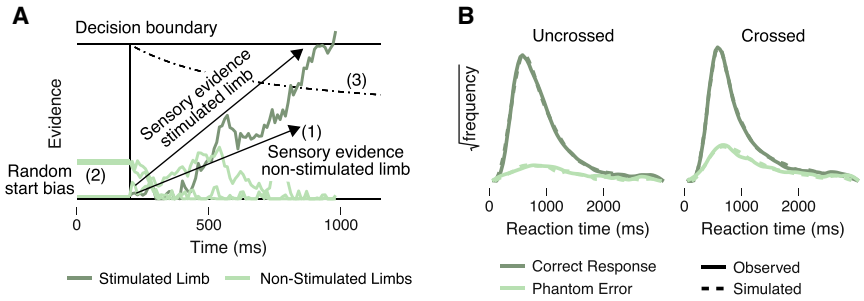

Figure 4. Evidence Accumulation in One-Stimulus Trials

(A) Model basics: in the model, noisy evidence is accumulated separately for each of the four limbs (green, stimulated limb; light green, non-stimulated limbs). The limb-choice response is given when the accumulated evidence for one of the limbs has reached the decision boundary. The four accumulators inhibit each other, with inhibition strength relative to their accumulated evidence, and they lose a fraction of the accumulated evidence in every time step (LCAs, leaky, competing accumulators [22]). Evidence accumulation starts after a random delay (vertical line), reflecting non-decision components in reaction times [23]; the drift rate (average incoming sensory evidence per time unit) of the stimulated limb (steeper arrow) is fixed to 1, and the noise (causing random fluctuations across time in the evidence signals) is Gaussian distributed and identical across accumulators. Model variants: we investigated the role of sensory and decision-making processes for the emergence of phantom errors by varying the respective components of the model. The final model was chosen based on its superior fit to the reaction time distributions for correct and phantom-error responses in one-stimulus trials of experiment 2. The best model comprised (1) positive sensory evidence toward a non-stimulated limb, (2) random initial biases, and (3) a constant decision boundary. (1) Sensory evidence toward non-stimulated limbs was implemented by means of non-zero drift rates; that is, one of the accumulators that represented non-stimulated limbs received positive evidence at each time step. The strength of this evidence signal (drift rate; less steep arrow) was a fraction of the drift rate for the stimulated limb. Additionally, the strength of all evidence signals varied randomly across trials. Including incoming sensory evidence for a non-stimulated limb proved necessary to mimic the frequency of phantom errors and correct responses across reaction times. (2) To implement initial biases toward random limbs, each limb's evidence accumulation process started with a random positive value of accumulated evidence (random start bias). This starting bias varied randomly across limbs and trials. For crossed conditions, the best-fitting model additionally comprised a trial-independent starting bias of 5% (threshold units) toward one non-stimulated limb. Such a fixed starting bias might represent evidence gathered before the start of the modeled evidence accumulation process [24, 25]. (3) A constant decision boundary (solid horizontal line) ensures that every response is based on the same amount of evidence. Such a constant decision criterion fitted the data better than a collapsing decision boundary (dot-dashed line) [26], which in turn formalizes an urgency to choose one of the four limbs by the end of the trial.

(B) Simulated (dashed line) and observed (solid line) RT distributions for correct (green) and phantom-error (light green) responses in the single touch condition of experiment 2. Frequencies are power transformed with −2 for illustration purposes only. Model predictions are based on 10,000 trials simulated using the best fitting parameter set of the winning model; see Data S1F for a full list of parameter values. Parameters were fitted separately for data from uncrossed (left) and crossed (right) conditions.

DISCUSSION

Errors in the localization of tactile stimuli are known from illusions such as the cutaneous rabbit [27] and tactile funneling [28], where the perceived location is displaced several centimeters from the stimulus location. In contrast, the phantom errors we observed here reveal misattributions of touch toward non-stimulated limbs. Such tactile misattributions toward non-stimulated limbs have only been reported in amputees and neurological patients recovering from stroke [6–10].

On the sensory homunculus of primary somatosensory cortex (SI), neurons with receptive fields on different limbs are distant from each other [1], excluding overlapping representations in SI [29] as a source of phantom errors. However, the limbs are represented in close proximity in secondary somatosensory areas [30–32], and cortically-distant limb representations in several somatosensory areas are interconnected via subcortical pathways [33–35]. Spreading of activation along such neural connections could explain phantom errors, analogous to accounts of tactile referral in amputees and neurological patients [8, 36]. Alternatively, the tactile—like the visual [37, 38]—system might abstract from topographic representations and encode tactile locations with respect to categories such as the type (hand or foot) or body side (left or right) of the touched limb. Indeed, posterior parietal regions represent body parts, body sides, and motor actions in a partially mixed fashion [39]. Moreover, neural activity in parietal brain regions has been associated with evidence accumulation models such as those used here [40]. Notably, the possibility that phantom errors arise outside of early sensory brain regions is compatible with their apparent perceptual similarity to errors indicating a touched limb; whereas SI activation does not necessarily elicit tactile sensations [41], activation in parietal and frontal areas is correlated with tactile awareness [42, 43]. In sum, both accounts, interconnected limb representations in somatosensory areas as well as categorical representations of the touched limb, can explain tactile percepts at untouched limbs.

Phantom errors provide new insight into the information used to identify a touched limb. Touch was erroneously attributed to limbs of the same limb type or body side as the correct limb and to limbs currently residing at the stimulated limb's canonical side of external space. These three spatial-tactile representations accounted for all phantom errors, including increased phantom-error rates with crossed limbs. Similar crossing effects have previously been interpreted as evidence for external-spatial coding of touch (reviews in [3–5, 44, 45]), given that errors varied with external-spatial limb location. Unlike previous studies, our paradigm was able to dissociate the external-spatial locations of touched and reported limbs. Phantom errors did not depend on the external-spatial location of the touched limb, implying that touch was attributed to a limb independent of its external-spatial location. Thus, our results imply that the influence of limb posture on the attribution of touch to the limbs [11–13, 15, 46–53] is not necessarily indicative of external-spatial coding of touch. Touch to crossed hands not only is regularly confused with touch to the other hand but also facilitates visual discrimination judgments next to the other hand [14] and tactile discrimination responses with the foot corresponding to the other hand [54, 55]. Thus, several lines of evidence indicate a canonical or posture-independent spatial representation of touch. The

present results imply that this canonical spatial representation does not reflect a body coordinate but extends across hands and feet momentarily placed in the corresponding hemispace. In sum, our findings support the notion that when attributing touch to the limbs, crossing effects arise due to an automatic activation of the touched limb's canonical side of external space.

Humans can discriminate tactile locations in external space [2]. This information could theoretically be used to attribute touch to a limb. Yet, identification of the touched limb requires categorization rather than precise computation of a tactile location. Body-related, categorical spatial representations such as limb type and body side correspond inherently to the categorical nature of the task and provide all information necessary to identify the touched limb. Notably, our results suggest that the limbs' locations in space are established correctly, given that response limbs were chosen according to their external position. Thus, external-spatial localization of a touched limb might proceed without determining the external-spatial location of the touch itself. In contrast, external-spatial representations of touch likely serve tactile localization in continuous external space, for example, to guide precise movements, such as swatting a mosquito or scratching a bite.

In conclusion, tactile percepts can arise at body locations distant from the stimulus's location in somatotopic or external-spatial maps. Across five experiments, attribution of touch to a limb relied on the stimulated limb's type, body side, and canonical side of external space. The limbs' locations in external space influenced limb choices, but they did so independent of stimulus location, incompatible with the use of external-spatial tactile representations. Attribution of touch to a limb might occur based on categories that characterize the touched limb rather than on continuous, physical coordinates within a somatotopic or external-spatial map.

STAR★METHODS

Detailed methods are provided in the online version of this paper and include the following:

- KEY RESOURCES TABLE
- CONTACT FOR REAGENT AND RESOURCE SHARING
- EXPERIMENTAL MODEL AND SUBJECT DETAILS
- METHOD DETAILS
  - Apparatus and Stimuli
  - Tasks
  - Design and Procedure
- QUANTIFICATION AND STATISTICAL ANALYSIS
  - Response categories
  - Pattern of phantom errors – within experiments
  - Pattern of phantom errors – within experiments II
  - Pattern of phantom errors – between experiments
  - Reaction times
  - Modeling
- DATA AND SOFTWARE AVAILABILITY

SUPPLEMENTAL INFORMATION

Supplemental Information can be found with this article online at https://doi.org/10.1016/j.cub.2019.02.060.

ACKNOWLEDGMENTS

Our work was supported by the German Research Foundation (DFG) with an Emmy Noether grant to T.H. (He 6368/1-1), a research fellowship grant to S.B. (BA 5600/1-1), a training grant to S.B. (CINACS, DFG GRK 1247/1 and 1247/2), and Leibniz award money to B.R. (Ro 2625/10-1) as well as by the University of Hamburg with a post-doctoral fellowship to S.B. We thank Franziska Rudzik, Lisa Thomaschewski, Katharina Werner, Lara Pleil, Nadine Blöcher, May-Britt Gerlach, Frederick Thiemer, and Christian Seegelke for help with data acquisition as well as Michael S. Landy, Marisa Carrasco, and Rachel Denison for helpful comments on a previous version of the manuscript.

AUTHOR CONTRIBUTIONS

Conceptualization, S.B. and T.H.; Methodology, S.B.; Software, S.B.; Formal Analysis and Modeling, S.B.; Investigation, S.B.; Writing – Original Draft, S.B. and T.H.; Writing – Review & Editing, S.B., T.H., and B.R.; Funding Acquisition, S.B., T.H., and B.R.; Resources, T.H. and B.R.; Visualization, S.B.; Supervision, S.B. and T.H.

DECLARATION OF INTERESTS

The authors declare no competing interests.

Received: October 30, 2017
Revised: February 15, 2019
Accepted: February 27, 2019
Published: April 4, 2019

REFERENCES

1. Penfield, W., and Rasmussen, T. (1950). The Cerebral Cortex of Man; a Clinical Study of Localization of Function (Macmillan).
2. Azañón, E., Longo, M.R., Soto-Faraco, S., and Haggard, P. (2010). The posterior parietal cortex remaps touch into external space. Curr. Biol. *20*, 1304–1309.
3. Medina, J., and Coslett, H.B. (2010). From maps to form to space: touch and the body schema. Neuropsychologia *48*, 645–654.
4. Longo, M.R., Azañón, E., and Haggard, P. (2010). More than skin deep: body representation beyond primary somatosensory cortex. Neuropsychologia *48*, 655–668.
5. Badde, S., and Heed, T. (2016). Towards explaining spatial touch perception: weighted integration of multiple location codes. Cogn. Neuropsychol. *33*, 26–47.
6. Borsook, D., Becerra, L., Fishman, S., Edwards, A., Jennings, C.L., Stojanovic, M., Papinicolas, L., Ramachandran, V.S., Gonzalez, R.G., and Breiter, H. (1998). Acute plasticity in the human somatosensory cortex following amputation. Neuroreport *9*, 1013–1017.
7. Grüsser, S.M., Mühlnickel, W., Schaefer, M., Villringer, K., Christmann, C., Koeppe, C., and Flor, H. (2004). Remote activation of referred phantom sensation and cortical reorganization in human upper extremity amputees. Exp. Brain Res. *154*, 97–102.
8. Medina, J., and Rapp, B. (2008). Phantom tactile sensations modulated by body position. Curr. Biol. *18*, 1937–1942.
9. Sathian, K. (2000). Intermanual referral of sensation to anesthetic hands. Neurology *54*, 1866–1868.
10. Ramachandran, V.S., and Hirstein, W. (1998). The perception of phantom limbs. The D. O. Hebb lecture. Brain *121*, 1603–1630.
11. Yamamoto, S., and Kitazawa, S. (2001). Reversal of subjective temporal order due to arm crossing. Nat. Neurosci. *4*, 759–765.
12. Shore, D.I., Spry, E., and Spence, C. (2002). Confusing the mind by crossing the hands. Brain Res. Cogn. Brain Res. *14*, 153–163.
13. Schicke, T., and Röder, B. (2006). Spatial remapping of touch: confusion of perceived stimulus order across hand and foot. Proc. Natl. Acad. Sci. USA *103*, 11808–11813.

14. Azañón, E., and Soto-Faraco, S. (2008). Changing reference frames during the encoding of tactile events. Curr. Biol. *18*, 1044–1049.
15. Badde, S., Heed, T., and Röder, B. (2016). Integration of anatomical and external response mappings explains crossing effects in tactile localization: a probabilistic modeling approach. Psychon. Bull. Rev. *23*, 387–404.
16. Reed, J.L., Qi, H.-X., and Kaas, J.H. (2011). Spatiotemporal properties of neuron response suppression in owl monkey primary somatosensory cortex when stimuli are presented to both hands. J. Neurosci. *31*, 3589–3601.
17. D'Amour, S., and Harris, L.R. (2014). Vibrotactile masking through the body. Exp. Brain Res. *232*, 2859–2863.
18. Avanzini, P., Pelliccia, V., Lo Russo, G., Orban, G.A., and Rizzolatti, G. (2018). Multiple time courses of somatosensory responses in human cortex. Neuroimage *169*, 212–226.
19. Fleming, S.M., and Frith, C.D., eds. (2014). The Cognitive Neuroscience of Metacognition (Springer).
20. Kiani, R., Corthell, L., and Shadlen, M.N. (2014). Choice certainty is informed by both evidence and decision time. Neuron *84*, 1329–1342.
21. Koriat, A. (2012). The self-consistency model of subjective confidence. Psychol. Rev. *119*, 80–113.
22. Usher, M., and McClelland, J.L. (2001). The time course of perceptual choice: the leaky, competing accumulator model. Psychol. Rev. *108*, 550–592.
23. Ratcliff, R., Smith, P.L., Brown, S.D., and McKoon, G. (2016). Diffusion decision model: current issues and history. Trends Cogn. Sci. *20*, 260–281.
24. Mulder, M.J., Wagenmakers, E.-J., Ratcliff, R., Boekel, W., and Forstmann, B.U. (2012). Bias in the brain: a diffusion model analysis of prior probability and potential payoff. J. Neurosci. *32*, 2335–2343.
25. de Lange, F.P., Rahnev, D.A., Donner, T.H., and Lau, H. (2013). Prestimulus oscillatory activity over motor cortex reflects perceptual expectations. J. Neurosci. *33*, 1400–1410.
26. Ditterich, J. (2006). Evidence for time-variant decision making. Eur. J. Neurosci. *24*, 3628–3641.
27. Geldard, F.A., and Sherrick, C.E. (1972). The cutaneous "rabbit": a perceptual illusion. Science *178*, 178–179.
28. von Békésy, G. (1967). Sensory Inhibition (Princeton University Press).
29. Schweizer, R., Maier, M., Braun, C., and Birbaumer, N. (2000). Distribution of mislocalizations of tactile stimuli on the fingers of the human hand. Somatosens. Mot. Res. *17*, 309–316.
30. Fitzgerald, P.J., Lane, J.W., Thakur, P.H., and Hsiao, S.S. (2004). Receptive field properties of the macaque second somatosensory cortex: evidence for multiple functional representations. J. Neurosci. *24*, 11193–11204.
31. Taoka, M., Toda, T., Hihara, S., Tanaka, M., Iriki, A., and Iwamura, Y. (2016). A systematic analysis of neurons with large somatosensory receptive fields covering multiple body regions in the secondary somatosensory area of macaque monkeys. J. Neurophysiol. *116*, 2152–2162.
32. Beauchamp, M.S., Yasar, N.E., Kishan, N., and Ro, T. (2007). Human MST but not MT responds to tactile stimulation. J. Neurosci. *27*, 8261–8267.
33. Tamè, L., Braun, C., Lingnau, A., Schwarzbach, J., Demarchi, G., Li Hegner, Y., Farnè, A., and Pavani, F. (2012). The contribution of primary and secondary somatosensory cortices to the representation of body parts and body sides: an fMRI adaptation study. J. Cogn. Neurosci. *24*, 2306–2320.
34. Tal, Z., Geva, R., and Amedi, A. (2017). Positive and negative somatotopic bold responses in contralateral versus ipsilateral penfield homunculus. Cereb. Cortex *27*, 962–980.
35. Tamè, L., Pavani, F., Papadelis, C., Farnè, A., and Braun, C. (2015). Early integration of bilateral touch in the primary somatosensory cortex. Hum. Brain Mapp. *36*, 1506–1523.
36. Makin, T.R., and Bensmaia, S.J. (2017). Stability of sensory topographies in adult cortex. Trends Cogn. Sci. *21*, 195–204.
37. Freedman, D.J., and Assad, J.A. (2009). Distinct encoding of spatial and nonspatial visual information in parietal cortex. J. Neurosci. *29*, 5671–5680.
38. Rishel, C.A., Huang, G., and Freedman, D.J. (2013). Independent category and spatial encoding in parietal cortex. Neuron *77*, 969–979.
39. Zhang, C.Y., Aflalo, T., Revechkis, B., Rosario, E.R., Ouellette, D., Pouratian, N., and Andersen, R.A. (2017). Partially mixed selectivity in human posterior parietal association cortex. Neuron *95*, 697–708.e4.
40. O'Connell, R.G., Shadlen, M.N., Wong-Lin, K., and Kelly, S.P. (2018). Bridging neural and computational viewpoints on perceptual decision-making. Trends Neurosci. *41*, 838–852.
41. de Lafuente, V., and Romo, R. (2005). Neuronal correlates of subjective sensory experience. Nat. Neurosci. *8*, 1698–1703.
42. Schubert, R., Blankenburg, F., Lemm, S., Villringer, A., and Curio, G. (2006). Now you feel it–now you don't: ERP correlates of somatosensory awareness. Psychophysiology *43*, 31–40.
43. Gallace, A., and Spence, C. (2008). The cognitive and neural correlates of "tactile consciousness": a multisensory perspective. Conscious. Cogn. *17*, 370–407.
44. Heed, T., Buchholz, V.N., Engel, A.K., and Röder, B. (2015). Tactile remapping: from coordinate transformation to integration in sensorimotor processing. Trends Cogn. Sci. *19*, 251–258.
45. Heed, T., and Azañón, E. (2014). Using time to investigate space: a review of tactile temporal order judgments as a window onto spatial processing in touch. Front. Psychol. *5*, 76.
46. Takahashi, T., Kansaku, K., Wada, M., Shibuya, S., and Kitazawa, S. (2013). Neural correlates of tactile temporal-order judgment in humans: an fMRI study. Cereb. Cortex *23*, 1952–1964.
47. Badde, S., Röder, B., and Heed, T. (2014). Multiple spatial representations determine touch localization on the fingers. J. Exp. Psychol. Hum. Percept. Perform. *40*, 784–801.
48. Badde, S., Röder, B., and Heed, T. (2015). Flexibly weighted integration of tactile reference frames. Neuropsychologia *70*, 367–374.
49. Azañón, E., Stenner, M.-P., Cardini, F., and Haggard, P. (2015). Dynamic tuning of tactile localization to body posture. Curr. Biol. *25*, 512–517.
50. Azañón, E., Mihaljevic, K., and Longo, M.R. (2016). A three-dimensional spatial characterization of the crossed-hands deficit. Cognition *157*, 289–295.
51. Azañón, E., Radulova, S., Haggard, P., and Longo, M.R. (2016). Does the crossed-limb deficit affect the uncrossed portions of limbs? J. Exp. Psychol. Hum. Percept. Perform. *42*, 1320–1331.
52. Heed, T., Backhaus, J., Röder, B., and Badde, S. (2016). Disentangling the external reference frames relevant to tactile localization. PLoS ONE *11*, e0158829.
53. Badde, S., Röder, B., and Bruns, P. (2018). Task-irrelevant sounds influence both temporal order and apparent-motion judgments about tactile stimuli applied to crossed and uncrossed hands. Atten. Percept. Psychophys. *80*, 773–783.
54. Medina, J., McCloskey, M., Coslett, H.B., and Rapp, B. (2014). Somatotopic representation of location: evidence from the Simon effect. J. Exp. Psychol. Hum. Percept. Perform. *40*, 2131–2142.
55. Ruzzoli, M., and Soto-Faraco, S. (2017). Modality-switching in the Simon task: the clash of reference frames. J. Exp. Psychol. Gen. *146*, 1478–1497.
56. R Core Team (2013). R: A language and environment for statistical computing (R Foundation for Statistical Computing).
57. Bates, D., Mächler, M., Bolker, B., and Walker, S. (2015). Fitting linear mixed-effects models using lme4. J. Stat. Softw. *67*, 1–48.
58. Wickham, H. (2016). ggplot2: Elegant Graphics for Data Analysis (Springer).

STAR★METHODS

KEY RESOURCES TABLE

REAGENT or RESOURCE	SOURCE	IDENTIFIER
Deposited Data		
Limb choice responses in Experiments 1-5	GitHub	https://github.com/StephBadde/HaendeFuessePhantomErrors
Software and Algorithms		
Presentation 14.5 (experimental control)	Neurobehavioral Systems, Albany, CA, USA	https://www.neurobs.com
R 3.5.0 (statistical analysis and modeling)	[56]	https://cran.r-project.org
lme4 package 1.1-12 (Poisson and binomial models)	[57]	https://cran.r-project.org/web/packages/lme4/index.html
ggplot2 package 2.2.1 (graphics)	[58]	https://cran.r-project.org/web/packages/ggplot2/index.html
Other		
Oticon Bone conducter, type BC 461-012 (tactile stimulation)	Oticon Ltd, Milton Keynes, UK	N/A

CONTACT FOR REAGENT AND RESOURCE SHARING

Further information and requests for resources should be directed to and will be fulfilled by the Lead Contact, Stephanie Badde (stephanie.badde@nyu.edu).

EXPERIMENTAL MODEL AND SUBJECT DETAILS

Twenty students from the University of Hamburg (all right-handed, 5 male, 20-31 years old, mean 23 years) participated in Experiment 1; sixteen students from the University of Hamburg (all right-handed, 4 male, 19-34 years old, mean 25 years) took part in Experiment 2; eighteen students from the University of Bielefeld participated in Experiment 3 (16 right-handed, 7 male, 19-29 years old, mean 23 years); sixteen students from the University of Hamburg (all right-handed, 3 male, 19-40 years old, mean 25 years) participated in Experiment 4; twelve students from the University of Bielefeld participated in Experiment 5 (11 right-handed, 9 male, 19-29 years old, mean 24 years). Sample sizes were determined based on previous experiments and no participant was excluded. All participants recruited for any of the experiments reported normal or corrected-to-normal vision and absence of tactile or motor impairments. They received course credit or were compensated with 7 Euro/hour. The study was approved by the ethical board of the German psychological society and all experiments were conducted in accordance with the general guidelines laid down in the Declaration of Helsinki. Participants gave written informed consent prior to the beginning of the experiment.

METHOD DETAILS

Apparatus and Stimuli

In Experiment 1, participants sat on the floor, resting their hands on transparent platforms 20 cm above their feet (Figure 1A). The hands were placed 20 cm apart, and the feet were vertically aligned with the hands. Participants' arms and legs were positioned either crossed or uncrossed. In the crossed conditions, a foam cushion was placed underneath the elbow of the upper arm and between the legs to avoid skin contact between crossed limbs. To avoid muscle fatigue, participants' backs and knees were supported by cushions, and the legs were bound loosely together with elastic band to prevent the knees from falling outward. Large response buttons were placed underneath both hands and fixed perpendicular to the floor next to both feet so that they could be pressed comfortably by a slight ankle movement. Tactile stimulators (Oticon bone conductors, type BC 461-012, Oticon Ltd, Milton Keynes, UK, sized about 1.6 × 1.0 × 0.8 cm) were taped to the webbing between thumb and index finger of the hands and the corresponding location on the feet, 2 cm proximal of the first metatarsalphalangeal joint. Stimuli consisted of 15 ms vibrations at a frequency of 167 Hz. Before each session, stimulation intensity of the four stimulators was adjusted by changing the pulse width of the rectangular stimulus signal. The intensity was set so that the perceived stimulus strength was distinctly suprathreshold and subjectively matched across all limbs. After each block, participants indicated whether the stimulus intensities needed to be readjusted.

Participants wore ear plugs and headphones playing white noise to shield off any auditory cues produced by the tactile stimulators. They were instructed to fixate on a central marker positioned so that hands and feet were located within participants' peripheral visual

field. Experiments were controlled by Presentation, version 14.5 (Neurobehavioral Systems, Albany, CA, USA), which interfaced with custom-built hardware to drive stimulators and record responses.

Apparatus and stimuli of Experiment 2 were identical to those of Experiment 1.

In Experiment 3, the distance between hands and feet was increased; participants sat on a chair and rested their hands on a transparent platform 70 cm above their feet. Otherwise, apparatus and stimuli of Experiment 3 were identical to those of Experiment 1.

In Experiment 4, a different response mode was employed. Participants wore cotton sleeves covering hands and feet. Each limb's sleeve had a different color (blue, green, red, yellow). Participants responded by calling out the colors to refer to the different limbs. Verbal responses were recorded using a microphone. Response time was measured using voice key, and the color response was manually recorded by the experimenter.

In Experiment 5, an additional response was required. Limb choice responses were again given by button press. After the button press, participants indicated verbally whether they had high or low confidence that the limb choice response was correct. As in Experiment 4, verbal responses were recorded using a microphone. Response time was measured using voice key, and the identity of the response was recorded online by the experimenter.

Tasks

In Experiments 1, 3, 4, and 5, two consecutive tactile stimuli, each to a different limb, were presented in each trial. Participants had to indicate which of the two tactile stimuli had occurred first by reporting the respective limb. Responses had to be withheld until the second tactile stimulus had been presented. No feedback was provided.

In Experiment 2, only one stimulus was presented in half of the trials. Participants reported the location of the first stimulus and ignored the second one if necessary.

In Experiment 5, the touch attribution task was followed by a confidence judgment, where participants indicated whether they had high or low confidence that the preceding limb choice response was correct.

Design and Procedure

Trials varied with respect to the posture of hands and feet, the stimulated limbs, and the stimulus onset asynchrony (SOA) of the stimuli. In Experiment 1, each combination of hand and foot posture (levels: uncrossed-uncrossed, uncrossed-crossed, crossed-uncrossed, and crossed-crossed), stimulated limbs (levels: all twelve combinations of one of the four limbs with one of the three other limbs), and SOA (levels; 50, 110, and 300 ms) was repeated twelve times. The experiment was divided into 48 blocks of 36 trials each. Participants completed the experiment in around six hours divided into 2 – 3 sessions of self-determined length usually conducted on different days. To check for influences of experiment duration, we predicted block-wise phantom-error rates from the position of the block within its session. No influence of the number of previously completed blocks on phantom-error rates was found (uncrossed: $\beta = 0.00$, $p = 0.175$; crossed: $\beta = 0.00$, $p = 0.468$).

Response times were restricted to 3000 ms. Trials were repeated at the end of the block if participants did not give a valid response (no response within the response time limits, 2.96% of trials; premature response, that is, response time shorter than 200 ms, 0.68% of trials; more than one response given, 1.98% of trials) and if the response was given with a non-stimulated limb (phantom error). We analyzed the data once including and once excluding repetitions, and verified that the pattern of phantom errors was independent of the repetitions (Spearman's rank correlation coefficient, $\rho = 0.976$, $p < .001$). Inter-trial intervals varied randomly from 2 to 2.5 s (uniform distribution). The stimulated limbs and SOA varied within blocks, each combination was presented once per block. Foot crossing status was changed every two blocks, and hand crossing status every four blocks. Condition order was counterbalanced across participants.

In the two-stimuli context of Experiment 2, each combination of posture, stimulated limbs, and SOA (levels: 110 and 300 ms) was repeated twelve times. In the one-stimulus context, each combination of stimulated limb (levels: left hand, right hand, left foot, and right foot) with posture was repeated 36 times. Experiment 2 comprised 48 blocks of 48 trials each and took around six hours to complete. The number of stimuli was varied within block, and the other conditions were varied as in Experiment 1.

Design and procedure of Experiment 3 were fully identical to those of Experiment 1.

The design of Experiment 4 was identical to that of Experiment 1. In Experiment 4, trials were not restricted in duration and the colored sleeves were re-attached after every change of posture to keep color assignment constant with respect to external space. Experiment 4 took around eight hours to complete.

The design of Experiment 5 was identical to that of Experiment 1. A tone served as a response cue for the confidence task and was presented 200-800 ms (uniform distribution) after the limb choice response was registered. Response times for button presses and for verbal confidence reports were restricted to 3000 ms. Experiment 5 took around eight hours to complete.

QUANTIFICATION AND STATISTICAL ANALYSIS

Response categories

Responses were coded with respect to the posture (uncrossed and crossed) and type (hand and foot) of the correct limb and in reference to response accuracy: (a) correct response with the limb that received the first stimulus; (b) erroneous response with the limb that received the second stimulus, a temporal order error; (c) erroneous response with a non-stimulated limb, a phantom error. As all experiments employed only a small set of SOAs, responses were pooled across SOAs. We further pooled across the identity of the

limb stimulated second, so that phantom errors could occur with equal probability at all three incorrect limbs. By doing so, we were able to analyze phantom errors independent of temporal order errors. Phantom errors were further categorized based on the relation between the limb that received the (first) tactile stimulus and the reported limb (Figure 1A). Phantom error responses could either be given with the limb homologous to the limb corresponding to the correct response (gray), or with a non-homologous limb (purple). Non-homologous limb responses could report either limbs of the same (light and dark red) or the opposite body side (light and dark blue), and the reported limb could be positioned either in the same (dark red and blue) or opposite (light red and blue) side of space as the correct limb.

Pattern of phantom errors – within experiments

To test which factors predicted the pattern of phantom errors, we fitted Poisson models, that is, generalized linear mixed models with Poisson distribution family and log link function, to participants' phantom-error counts.

The first model used the homology of limb type between correct and reported limb (levels: homologous and non-homologous) as well as the type (levels: hand and foot) and posture (levels: uncrossed and crossed) of the correct limb as fixed factors. The second model focused on phantom errors reporting non-homologous limbs. It differentiated between body side (levels: same and other body side) and side of space (levels: same and other side of external space) correspondences between correct and reported limb. The model simultaneously controlled for the posture of the correct limb. Thus, the first model addressed the limb type of the correct and the reported limb, and the second model the spatial relations between these two limbs. It was necessary to separate the two analyses, as these predictors are interdependent; phantom errors reporting a limb of the same type as the correct one by definition always report a limb from the other side of the body and located at the other side of space.

To test which factors predicted participants' confidence ratings in Experiment 5, we fitted logistic models, that is, generalized linear mixed models with binomial distribution family and a logit link function, to participants' binary confidence responses. The first model predicted confidence ratings from the reaction time and response type (correct response, temporal order error, and phantom error) of the rated button press. Reaction times were log-transformed to reduce the skewness of their distribution. Treatment contrasts were used to directly estimate the difference in confidence between two response types; the contrasts were re-leveled, and the model was re-evaluated to test the third pairing of response types. Two additional models predicted confidence ratings exclusively in trials in which the response was a phantom error. The first model used the limb type of the correct and the reported limb combined with posture of the correct limb and reaction times as predictors. The second model used body side and side of space combined with posture of the correct limb and reaction times of the limb choice response as predictors.

10,000 parametric bootstraps were performed for each model to estimate confidence intervals for every parameter and evaluate its significance. Significant interactions were followed up by sub-models.

Pattern of phantom errors – within experiments II

To analyze effects of the timing of the second stimulus onto the pattern of phantom errors across the limbs, we determined the number of phantom error responses per category (Figure 1A) and per posture of the correct limb separately for each SOA. To quantify the similarity of those categorical frequency distributions across SOA conditions, we calculated the rank correlation coefficient Spearman's rho for each pairing of SOAs and tested the resulting statistic against 0 by transforming the coefficient into a z-value (see Data S1C).

To analyze effects of the position of the second stimulus onto the pattern of phantom errors across the limbs, we coded the 12 different combinations of first and second stimulated limb according to their relation: the second touch could be located at the homologous limb or at a non-homologous limb of either the same or the other body side as the limb touched first. Direct comparisons of phantom-error frequencies across these conditions (second touch at (1) homologous limb, (2) non-homologous limb of the same body side, and (3) non-homologous limb of the other body side) were impossible due to a confound between the relative location of the second touch and error type. Each of the three conditions precludes a different type of phantom error. For example, if both tactile stimuli have been applied to the hands, phantom-error responses with a homologous limb cannot occur; if the stimuli have been applied to the right hand and foot, phantom-error responses with limbs of the same side of the body cannot occur. These errors are temporal order errors, the limb stimulated second is reported. To overcome this confound, we compared the rate of correct responses across the three different stimulation categories and the two postures. Significant interactions between posture of the correct limb and stimulus pair were followed-up by pairwise comparisons of stimulus conditions within each posture condition (see Data S1D).

Pattern of phantom errors – between experiments

Here, we determined the number of phantom-error responses per category (Figure 1A) and per posture of the correct limb for each experiment. The different stimulation contexts of Experiment 2 were treated as separate experiments. To quantify the similarity across experiments, we calculated Spearman's rho for each pairing of Experiment 1 with one of the other experiments.

With regard to Experiment 3, we were especially interested in the question of whether the effect of side of space on phantom errors was different from the corresponding effect in Experiment 1. To this aim, we fitted a Poisson model (predictors: posture of the correct limb, body side, side of space, and experiment (levels: Experiments 1 and 3)) to participants' individual counts of phantom-error responses with limbs non-homologous to the correct one.

Reaction times

For each participant, we determined the mode of the reaction time (RT) distribution based on Kernel densities estimated separately for each response type, that is, correct responses, temporal order errors, and phantom errors, and both postures of the correct limb. RT modes were analyzed with a repeated-measures ANOVA with factors response type and posture of the correct limb. Significant effects were followed-up using pairwise paired t tests (see Figure S2 and Data S1E for RT data).

Modeling

To test the role of perceptual and decision making processes for the emergence of phantom errors we fitted leaky, competing accumulator (LCA) models [27] to the RT distributions of correct and phantom-error responses in one-stimulus trials of Experiment 2. All models comprised one accumulator for each of the four limbs. Evidence accumulation stopped when one accumulator reached the decision bound. If none of the accumulators had reached the decision bound within the trial time of 3000 ms, the trial was deemed invalid. For model evaluation, time was discretized into 50 ms bins. We simulated 10,000 trials every time the model was evaluated. The model contained a reflective bound, that is, negative evidence was not allowed. In every time step dt/T the accumulated evidence ρ for a limb i was updated according to

$$dx_i = \left(\rho_i - \kappa x_i + \beta \sum_{j \neq i} x_j\right)\frac{dt}{T} + \xi\sqrt{\frac{dt}{T}},$$

where ξ is a Gaussian noise term (Equation 4 [27]). Across accumulators, the noise was independent and identically distributed with mean 0 and standard deviation σ_ξ. Each LCA model variant included the following parameters: $\beta \in [0, 1]$ the degree of mutual inhibition between the four accumulators, $\kappa \in [0, 1]$ the degree of evidence leakage from one time step to another, τ the threshold value serving as a decision boundary, t_{err} the non-decision time and σ_{terr} the spread of the non-decision time's random uniform variation, as well as σ_ξ the standard deviation of the Gaussian distributed processing noise of each accumulator. To scrutinize the processes involved in the generation of phantom errors, we additionally included subsets of the following parameters: ρ_i the strength of the input signal to a non-stimulated limb relative to the strength of the input signal to the stimulated limb, with the latter fixed to 1, σ_ρ the spread of a uniform distribution adding random variation across trials to the input signals of all four accumulators, b a shift in the degree of evidence for one or several accumulators at time 0, that is, a bias toward one or several limbs at the start of accumulation process given in threshold units, σ_b the spread of a uniform distribution adding random variation across trials to the starting evidence for each accumulator (again in threshold units), and two parameters characterizing a collapsing decision boundary [23], κ_τ the steepness of the decline as well as s the time point within a trial at which the decision boundary was reduced to half of the original threshold.

During parameter fitting, goodness-of-fit was quantified by means of χ^2 – values capturing the difference between the observed and the predicted number of correct and phantom responses in nine RT bins (boundaries at 0.025, 0.05, 0.15, 0.3, 0.5, 0.7, 0.85, 0.95, and 0.975 percentiles of the observed data; determined separately for correct and phantom-error responses). The parameter space was high-dimensional and non-monotonic with collinearities between some parameters. We employed a two-step approach to find the best fitting parameter set for each model variant. First, we conducted a grid-search to identify the ten best-fitting values for each subset of parameters that defined a model variant. Several million grid points were evaluated. Second, using these parameter sets as starting points we fitted the parameters using conditional maximization, that is, dividing the parameter space into disjunctive subsets, and iteratively optimizing the subsets of parameters using the Nelder-Mead algorithm while temporally fixing the other parameters. Within one iteration of the conditional maximization procedure, each simplex was run five times with equally spaced starting points. The best-fitting subset was chosen and fixed for the next iteration of the conditional maximization procedure. 200 iterations were run for each parameter set. Finally, the best fitting model across model variants was determined based on BIC values, which additionally account for the number of parameters of each model.

DATA AND SOFTWARE AVAILABILITY

Data is available on GitHub, https://github.com/StephBadde/HaendeFuessePhantomErrors.